Available online at www.sciencedirect.com
SCIENCE DIRECT®
Journal of Sound and Vibration 292 (2006) 987–998
JOURNAL OF SOUND AND VIBRATION
www.elsevier.com/locate/jsvi

Short Communication

Design of mechanical band-pass filters for energy scavenging

S.M. Shahruz*

Berkeley Engineering Research Institute, P.O. Box 9984, Berkeley, California 94709, USA

Received 13 May 2005; received in revised form 17 June 2005; accepted 31 August 2005
Available online 28 November 2005

Abstract

In this paper, the design of mechanical band-pass filters to be used in energy scavengers is studied. For such filters an ensemble of cantilever beams is proposed where at the tip of each beam a mass, known as the proof mass, is mounted. It is shown that such an ensemble can be made into a band-pass filter when dimensions of the beams and masses of the proof masses are chosen appropriately. A systematic procedure for designing mechanical band-pass filters is given. It is shown that the maximal frequency band of the band-pass filter is limited and cannot be chosen arbitrarily large: The frequency band is independent of dimensions of the beams and masses of the proof masses.

1. Introduction

Harvesting energy from the environment has been a desire and practice of the man. Throughout centuries, many devices and tools have been designed and made to generate power from natural resources, such as solar radiation, wind and air flow, tidal waves, temperature gradients in oceans, pressure variations, water flow, fossil and nuclear fuels, etc.; see, e.g., Refs. [1–5].

There is yet the concept of energy scavenging from the ambient which is receiving attention recently. Energy scavenging is commonly understood as the conversion of low-level ambient energy, which is usually neglected, into usable but small amount of energy; see, e.g., Refs. [6–13]. Some examples are: (1) kinetic energy of a human arm can be used to wind a wrist watch; (2) piezoelectric shoe inserts can convert energy of walking into electricity; (3) vibration in buildings, bridges, cars, trains, aircraft, ships, manufacturing tools, etc., can be converted into electricity to power micro-electronic devices. A device that scavenges energy efficiently from the environment is called an energy scavenger. Integration of energy scavengers and devices leads to energy self-sufficient devices where there is no need to replace their depleted power supplies. Examples of such devices are energy self-sufficient sensors to be used in large wireless sensor networks or inside the car tires.

In order to convert the ambient kinetic or vibrational energy into electricity, piezoelectric films are commonly incorporated in energy scavengers; see, e.g., Ref. [13] and the references therein. A typical energy scavenger consists of a cantilever beam on which a piezoelectric film and a mass are mounted; see Fig. 1. This device will be referred to as either the energy scavenger or the beam–mass system. When the scavenger is

*Tel.: +1 510 642 3248; fax: +1 510 642 1341.
E-mail address: shahruz@cal.berkeley.edu.

0022-460X/$ - see front matter © 2005 Elsevier Ltd. All rights reserved.
doi:10.1016/j.jsv.2005.08.018

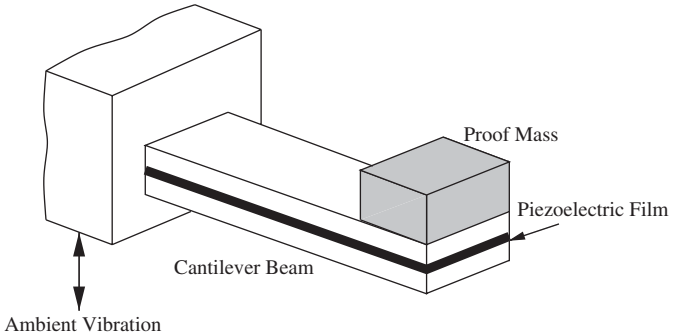

Fig. 1. A typical energy scavenger consists of a cantilever beam on which a piezoelectric film and a mass, known as the proof mass, are mounted.

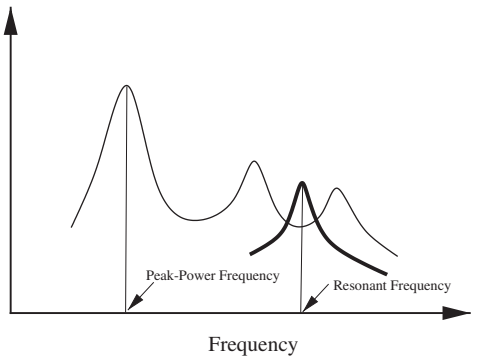

Fig. 2. The power spectral density of the signal generated by a vibration source (thin line) and the Bode magnitude plot of a mechanical band-pass filter (thick line). An energy scavenger is less efficient if its resonant frequency is not close to the peak-power frequency of the vibration source: The scavenger would not resonate.

mounted on a vibration source, say a panel, the cantilever beam would vibrate. The vibration of the beam is converted into electricity by the piezoelectric film. The mass on the cantilever beam is known as the proof mass. It is used to change the resonant (fundamental) frequency of the scavenger. Recall that the resonant frequency of a linear dynamical system is defined as the frequency at which the Bode magnitude plot corresponding to the system has the largest magnitude.

A vibration source generates a signal which is a function of time. To this function there corresponds a power spectral density which is a function of frequency. The frequency at which the power spectral density is the largest is called the peak-power frequency. When the resonant frequency of a scavenger matches the peak-power frequency of the vibration source to which it is attached, harvesting of energy is the most efficient. The scavenging efficiency is very low otherwise; for instance, in a situation such as that depicted in Fig. 2.

It is certainly possible to manufacture an energy scavenger the resonant frequency of which matches the peak-power frequency of a certain vibration source. It is, however, not feasible to manufacture as many energy scavengers as there are vibration sources with different peak-power frequencies. The range of peak-power frequencies of vibration sources can be determined via measurement; for instance, it could be between 100 and 200 Hz. Therefore, in order to scavenge energy efficiently, an energy scavenger should have sufficient bandwidth in the range of peak-power frequencies of vibrations sources. A device with such a property is nothing but a mechanical band-pass filter with a Bode magnitude plot such as that shown in Fig. 3.

In this paper, the goal is to design energy scavengers that can efficiently harvest energy from a variety of vibration sources with different peak-power frequencies. In other words, the goal is to design mechanical band-pass filters. The organization of the paper is as follows. In Section 2, a mathematical model is obtained to describe the transversal vibration of a beam–mass system. In Section 3, an ensemble of beam–mass systems

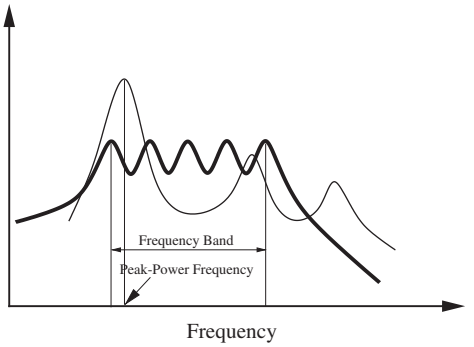

Fig. 3. The power spectral density of the signal generated by a vibration source (thin line) and the Bode magnitude plot of a mechanical band-pass filter (thick line). A band-pass filter can scavenge energy from vibration sources the peak-power frequencies of which are within the frequency band of the filter.

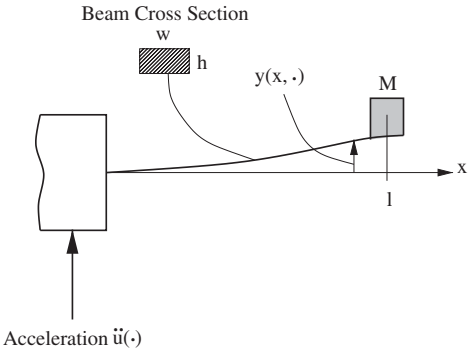

Fig. 4. A schematic of a beam with a proof mass at its tip. The vibration source exerts the acceleration $\ddot{u}(\cdot)$. The transversal displacement of the beam at an $x \in [0, l]$ and a $t \geqslant 0$ is denoted by $y(x, t)$.

is considered. It is shown that such an ensemble can be made into a band-pass filter when dimensions of the beams and masses of the proof masses are chosen appropriately. A systematic procedure for designing mechanical band-pass filters is given. It is shown that the frequency band of the band-pass filter is limited and cannot be chosen arbitrarily large: The maximal frequency band is independent of dimensions of the beams and masses of the proof masses. Examples are presented throughout the paper.

2. A mathematical model of vibrating beam-mass systems

In Fig. 4, consider a schematic of the beam–mass system shown in Fig. 1. The length, width, and thickness of the beam are denoted by l, w, and h, respectively. The mass density and the modulus of elasticity of the beam are denoted by ρ and E, respectively. The proof mass at the tip of the beam is assumed to be a point mass of mass M. The vibration source, on which the cantilever beam is mounted, exerts the acceleration $\ddot{u}(\cdot)$. Due to this external input, the beam vibrates transversally. The transversal displacement of the beam at an $x \in [0, l]$ and a $t \geqslant 0$ is denoted by $y(x, t) \in \mathbb{R}$.

With this setup, a mathematical model describing the dynamics of the beam–mass system is sought. It is possible to derive a linear partial differential equation to describe the evolution of the beam displacement, $y(x, t)$, for all $x \in [0, l]$ and $t \geqslant 0$. Instead of a partial differential equation, a simpler and mathematically tractable model is preferred. One such model is the generalized single-degree-of-freedom (sdof) system corresponding to the beam–mass system; see, e.g., Ref. [14, pp. 140–145].

To develop the generalized sdof system, the transversal displacement of the beam is written as

$$y(x, t) = \phi(x)q(t), \tag{1}$$

for all $x \in [0, l]$ and $t \geqslant 0$, where the real- and scalar-valued function $x \mapsto \phi(x)$ is a known trial (shape) function and the real- and scalar-valued function $t \mapsto q(t)$ is an unknown (generalized coordinate) function.

The trial function is chosen to be the first mode of the free transversal vibration of the beam–mass system in Fig. 4, given by (see, Ref. [15, pp. 186–188]):

$$\phi(x) = \sin\left(\lambda(\alpha)\left(\frac{x}{l}\right)\right) - \sinh\left(\lambda(\alpha)\left(\frac{x}{l}\right)\right) - \frac{\sinh\lambda(\alpha) + \sinh\lambda(\alpha)}{\cos\lambda(\alpha) + \cosh\lambda(\alpha)}\left[\cos\left(\lambda(\alpha)\left(\frac{x}{l}\right)\right) - \cosh\left(\lambda(\alpha)\left(\frac{x}{l}\right)\right)\right], \tag{2}$$

for all $x \in [0, l]$, where λ depends on $\alpha := M/\rho whl$. Using the first two terms in the series expansions of $\sin(\lambda(\alpha)(x/l))$, $\sinh(\lambda(\alpha)(x/l))$, $\cos(\lambda(\alpha)(x/l))$, and $\cosh(\lambda(\alpha)(x/l))$ (see, e.g., Ref. [16]) in Eq. (2), the trial function is approximated by

$$\phi(x) = a(\alpha)\left(\frac{x}{l}\right)^2 - b(\alpha)\left(\frac{x}{l}\right)^3, \tag{3}$$

for all $x \in [0, l]$, where

$$a(\alpha) = \frac{\sin\lambda(\alpha) + \sinh\lambda(\alpha)}{\cos\lambda(\alpha) + \cosh\lambda(\alpha)}\lambda^2(\alpha), \quad b(\alpha) = \frac{1}{3}\lambda^3(\alpha). \tag{4}$$

Using the value of α and the corresponding $\lambda(\alpha)$ in Ref. [15, p. 188, Table 6.7(a)], $a(\alpha)$ and $b(\alpha)$ can be computed for all $\alpha \geqslant 0$. It can be easily verified that for any $\alpha \geqslant 0$, the functions in Eqs. (2) and (3) are very close to each other over the interval $[0, l]$ by plotting their graphs. In the following, for the sake of brevity, the dependence of λ, a, b, $x \mapsto \phi(x)$, and other functions on α is not pedantically stated everywhere.

In developing the generalized sdof system, the generalized mass, the generalized flexural stiffness, and the generalized effective load corresponding to the beam–mass system should be known; see, e.g., Ref. [14, p. 143]. Such quantities are computed in the following.

The generalized mass is

$$m = \int_0^l \rho wh\phi^2(x)\,\mathrm{d}x + M\phi^2(l). \tag{5}$$

Using Eq. (3) in Eq. (5), it is concluded that

$$m = (a-b)^2 M + \left(\frac{a^2}{5} - \frac{2ab}{6} + \frac{b^2}{7}\right)\rho whl. \tag{6}$$

The generalized flexural stiffness is

$$k = \int_0^l EI\left(\frac{\mathrm{d}^2\phi(x)}{\mathrm{d}x^2}\right)^2 \mathrm{d}x, \tag{7}$$

where $I = wh^3/12$ is the second moment of area of the beam cross-section. Using Eq. (3) in Eq. (7), it follows that

$$k = \frac{(a^2 - 3ab + 3b^2)Ewh^3}{3l^3}. \tag{8}$$

The generalized effective load in the absence of gravity is

$$f_{\mathrm{eff}}(t) = -\left(\int_0^l \rho wh\phi(x)\,\mathrm{d}x + M\phi(l)\right)\ddot{u}(t), \tag{9}$$

for all $t \geqslant 0$. Using Eq. (3) in Eq. (9), it is concluded that

$$f_{\text{eff}}(t) = -\left((a-b)M + \left(\frac{a}{3} - \frac{b}{4}\right)\rho whl\right)\ddot{u}(t), \tag{10}$$

for all $t \geqslant 0$.

Using Eqs. (6), (8), and (10) in Eq. (8–15) in Ref. [14, p. 143], the generalized sdof system corresponding to the beam–mass system is obtained as the following second-order ordinary differential equation:

$$[a_1(\alpha)M + a_2(\alpha)\rho whl]\ddot{q}(t) + \frac{a_3(\alpha)Ewh^3}{3l^3}q(t) = -[a_4(\alpha)M + a_5(\alpha)\rho whl]\ddot{u}(t),$$

$$q(0) = 0, \quad \dot{q}(0) = 0, \tag{11}$$

all $t \geqslant 0$, where

$$a_1(\alpha) \coloneqq [a(\alpha) - b(\alpha)]^2, \quad a_2(\alpha) \coloneqq \frac{a^2(\alpha)}{5} - \frac{2a(\alpha)b(\alpha)}{6} + \frac{b^2(\alpha)}{7}, \tag{12a}$$

$$a_3(\alpha) \coloneqq a^2(\alpha) - 3a(\alpha)b(\alpha) + 3b^2(\alpha), \tag{12b}$$

$$a_4(\alpha) \coloneqq a(\alpha) - b(\alpha), \quad a_5(\alpha) \coloneqq \frac{a(\alpha)}{3} - \frac{b(\alpha)}{4}. \tag{12c}$$

Using the value of α and the corresponding $\lambda(\alpha)$ in Ref. [15, p. 188, Table 6.7(a)], $a(\alpha)$ and $b(\alpha)$ in Eq. (4) can be computed for all $\alpha \geqslant 0$. Having these quantities computed, it can be verified numerically that $0 < a_i(\alpha) < \infty$ for all $\alpha \geqslant 0$ and $i = 1, 2, \ldots, 5$.

The unique solution of system (11) for $t \mapsto q(t)$ can be obtained. When this solution is substituted into Eq. (1), the transversal displacement of the undamped beam is (approximately) obtained.

In order to take into account the energy dissipation in the beam–mass system, a viscous damping term is added to the left-hand side of Eq. (11). The result is

$$m\ddot{q}(t) + c\dot{q}(t) + kq(t) = -f\ddot{u}(t), \quad q(0) = 0, \quad \dot{q}(0) = 0, \tag{13}$$

for all $t \geqslant 0$, where c is a positive real number known as the damping coefficient, and

$$m \coloneqq a_1(\alpha)M + a_2(\alpha)\rho whl, \quad k \coloneqq \frac{a_3(\alpha)Ewh^3}{3l^3}, \quad f \coloneqq a_4(\alpha)M + a_5(\alpha)\rho whl. \tag{14}$$

The undamped natural frequency and the damping ratio corresponding to both system (13) and the beam–mass system are defined, respectively, as

$$\omega_n \coloneqq \left(\frac{k}{m}\right)^{1/2}, \quad \xi \coloneqq \frac{c}{2(mk)^{1/2}}. \tag{15a,b}$$

The unique solution of system (13) for $t \mapsto q(t)$ can be obtained. When this solution is substituted into Eq. (1), the transversal displacement of the damped beam is (approximately) obtained. Having the values of $a(\alpha)$ and $b(\alpha)$ for all $\alpha \geqslant 0$, it can be easily verified that the function $x \mapsto \phi(x)$ in Eq. (3) is monotonically increasing over the interval $[0, l]$ for all $\alpha \geqslant 0$. Thus, $x \mapsto \phi(x)$ attains its maximum at $x = l$ for all $\alpha \geqslant 0$. Therefore, for any $\alpha \geqslant 0$, the absolute value of displacement of the tip of the beam, $|y(l, t)|$, is the largest at every $t \geqslant 0$.

By applying the Laplace transform to Eq. (1), it follows that

$$y(x, s) = \phi(x)q(s), \tag{16}$$

for all $x \in [0, l]$, where $y(x, s)$ and $q(s)$ are the Laplace transforms of $y(x, \cdot)$ and $q(\cdot)$, respectively. A transfer function, which relates the transversal displacement of the tip of the beam to the applied acceleration, is defined as

$$g_{\text{tip}}(s) \coloneqq \frac{y(l, s)}{\ddot{u}(s)}, \tag{17}$$

where $\ddot{u}(s)$ is the Laplace transforms of $\ddot{u}(\cdot)$. Using Eqs. (16), (3), (12c), and (13) in Eq. (17), it is concluded that

$$g_{\text{tip}}(s) = \frac{\phi(l)q(s)}{\ddot{u}(s)} = -\frac{a_4 f}{ms^2 + cs + k}. \tag{18}$$

The H_∞-norm of $g_{\text{tip}}(s)$ is defined as

$$\|g_{\text{tip}}\|_\infty := \max_{\omega \in \mathbb{R}} |g_{\text{tip}}(\mathrm{j}\omega)|, \tag{19}$$

where $\mathrm{j} = \sqrt{-1}$. The norm $\|g_{\text{tip}}\|_\infty$ corresponds to the (global) maximum of the Bode magnitude plot of the transfer function $g_{\text{tip}}(s)$.

It is well known that at the resonant frequency of the beam–mass system

$$\omega_r = \omega_n(1 - 2\xi^2)^{1/2}, \tag{20}$$

the magnitude $|g_{\text{tip}}(\mathrm{j}\omega)|$ attains its maximum given by

$$\|g_{\text{tip}}\|_\infty = \frac{a_4 f}{2\xi k(1 - \xi^2)^{1/2}}, \tag{21}$$

where ω_n and ξ are those in Eq. (15). When $0 < \xi \ll 1$, it follows that $\omega_r \approx \omega_n = (k/m)^{1/2}$ and $\|g_{\text{tip}}\|_\infty \approx a_4 f/(2\xi k)$. Thus, by Eq. (14), it is concluded that

$$\omega_r = \left(\frac{a_3(\alpha) E w h^3}{3[a_1(\alpha)M + a_2(\alpha)\rho w h l] l^3}\right)^{1/2}, \tag{22a}$$

$$\|g_{\text{tip}}\|_\infty = \frac{3a_4(\alpha)[a_4(\alpha)M + a_5(\alpha)\rho w h l] l^3}{2\xi a_3(\alpha) E w h^3}, \tag{22b}$$

for all $\alpha \geqslant 0$, where $a_1(\alpha), a_2(\alpha), \ldots, a_5(\alpha)$ are given in Eq. (12).

In the design of mechanical band-pass filters, the resonant frequency ω_r and the norm $\|g_{\text{tip}}\|_\infty$ will be used. An example is given in the following to illustrate the computation of these two quantities.

Example 2.1. Let the beam in Fig. 4 be made out of silver with the following material properties:

$$\rho = 10\,500\,\text{kg/m}^3, \quad E = 7.8 \times 10^{10}\,\text{N/m}^2, \quad \xi = 0.01. \tag{23}$$

Let the beam dimensions and the proof mass be

$$l = 0.04\,\text{m}, \quad w = 0.005\,\text{m}, \quad h = 0.001\,\text{m}, \tag{24a}$$

$$M = 0.0042\,\text{kg}. \tag{24b}$$

With this setup, $\alpha = M/\rho w h l = 2$. Therefore, from Ref. [15, p. 188, Table 6.7(a)], $\lambda = 1.076$. Using Eqs. (4), (12), (14), (15b), and (18), it follows that

$$g_{\text{tip}}(s) = -\frac{0.0302}{0.02843s^2 + 0.324s + 9229}. \tag{25}$$

The Bode magnitude plot of the transfer function in Eq. (25) is shown in Fig. 5.

Using Eqs. (4), (12), and (22), it is concluded that

$$\omega_r = 569.74\,\text{rad/s} = 90.68\,\text{Hz}, \quad \|g_{\text{tip}}\|_\infty = 1.6364 \times 10^{-4}\,\text{s}^2. \tag{26}$$

Note that the peak of the Bode magnitude plot in Fig. 5 is equal to $20\log_{10}\|g_{\text{tip}}\|_\infty$.

3. A mechanical band-pass filter

The goal of this section is to explore the possibility of designing a mechanical band-pass filter from an ensemble of beam–mass systems, such as that shown in Fig. 6. Conceivably, if dimensions of the beams and masses of the proof masses are chosen appropriately, then the device in Fig. 6 can function as a band-pass filter.

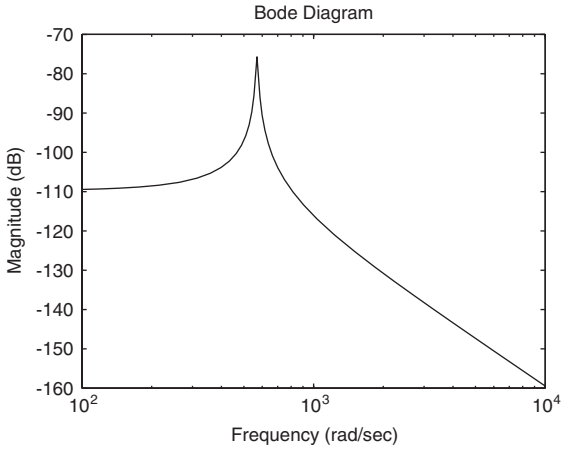

Fig. 5. The Bode magnitude plot of the transfer function corresponding to the beam–mass system in Example 2.1.

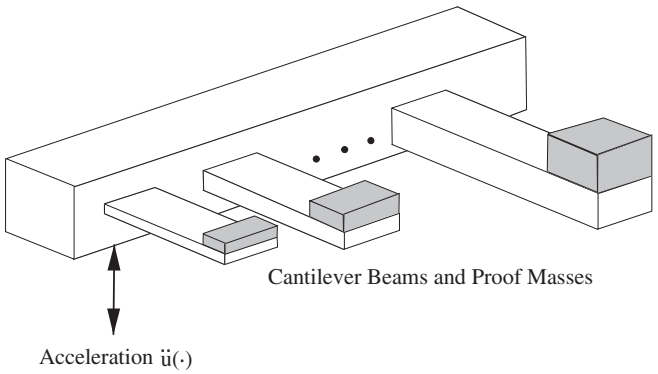

Fig. 6. An ensemble of cantilever beams with proof masses at their tips. When dimensions of the beams and masses of the proof masses are chosen appropriately, this ensemble can function as a band-pass filter.

Recall that Eq. (22) shows the dependence of the resonant frequency ω_r and the norm $\|g_{\text{tip}}\|_\infty$ on the beam dimensions and the proof mass. Using this equation, it is examined whether it is possible to choose beams with different dimensions and different proof masses such that: (i) resonant frequencies ω_r of the beam–mass systems are different from each other; (ii) norms $\|g_{\text{tip}}\|_\infty$ corresponding to all beam–mass systems assume a same constant value, say $\gamma^* > 0$. If the device in Fig. 7 satisfies conditions (i) and (ii), then it functions as a band-pass filter. In this case, the Bode magnitude plots of the transfer functions corresponding to the beam–mass systems would look like those in Fig. 7. An important question that arises is: What is the maximal achievable frequency band $(\omega_{\min}, \omega_{\max})$ over which $\|g_{\text{tip}}\|_\infty$ corresponding to each beam–mass system is equal to γ^*? As it will be shown in the following, this interval is limited and cannot be chosen arbitrarily large.

In Eq. (22b), the norm $\|g_{\text{tip}}\|_\infty$ is set equal to $\gamma^* > 0$. The result is

$$\gamma^* = \frac{3a_4(\alpha)[a_4(\alpha)M + a_5(\alpha)\rho whl]l^3}{2\xi a_3(\alpha)Ewh^3}, \tag{27}$$

for all $\alpha \geqslant 0$. Dimensions of the beams and masses of the proof masses should satisfy the equality constraint in Eq. (27), should the transfer functions $g_{\text{tip}}(s)$ corresponding to the beam–mass systems have their H_∞-norms equal to γ^*. Using the relation

$$M = \alpha\rho whl, \tag{28}$$

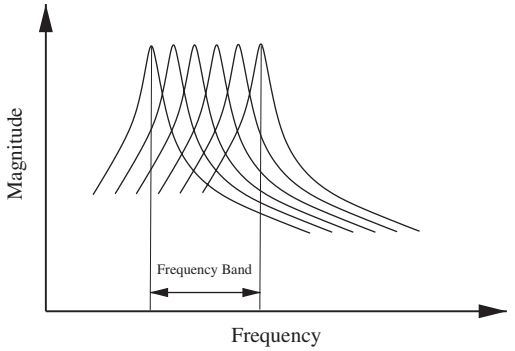

Fig. 7. The Bode magnitude plots of the transfer functions corresponding to the beam–mass systems of the device in Figure 6 when the device functions as a band-pass filter. The frequency band of the filter is denoted by $(\omega_{\min}, \omega_{\max})$.

Table 1
Values of two functions

α	$F(\alpha)$ in Eq. (31)	$G(\alpha)$ in Eq. (34)
0.00	0.8758	1.0949
0.03	0.8616	1.0694
0.05	0.8533	1.0540
0.10	0.8355	1.0212
0.15	0.8214	0.9936
0.20	0.8099	0.9698
0.25	0.8004	0.9489
0.35	0.7858	0.9134
0.50	0.7708	0.8705
0.75	0.7553	0.8170
1.00	0.7459	0.7768
1.50	0.7349	0.7187
2.00	0.7288	0.6774

in Eq. (27), it follows that

$$l^4 = \left(\frac{2a_3(\alpha)E\xi\gamma^*}{3a_4(\alpha)[\alpha a_4(\alpha) + a_5(\alpha)]\rho}\right)h^2, \tag{29}$$

for all $\alpha \geqslant 0$. Substituting Eqs. (28) and (29) into Eq. (22a), it is concluded that

$$\omega_r = \left(\frac{a_4(\alpha)[\alpha a_4(\alpha) + a_5(\alpha)]}{2[\alpha a_1(\alpha) + a_2(\alpha)]}\right)^{1/2}\left(\frac{1}{\xi\gamma^*}\right)^{1/2}, \tag{30}$$

for all $\alpha \geqslant 0$.

An important conclusion is drawn from Eq. (30) as follows. Let

$$F(\alpha) := \left(\frac{a_4(\alpha)[\alpha a_4(\alpha) + a_5(\alpha)]}{2[\alpha a_1(\alpha) + a_2(\alpha)]}\right)^{1/2}, \tag{31}$$

for all $\alpha \geqslant 0$. The scalar-valued function $\alpha \mapsto F(\alpha)$ appears on the right-hand side of Eq. (30). This function is evaluated by using the values of α and the corresponding $\lambda(\alpha)$ in Ref. [15, p. 188, Table 6.7(a)] and Eqs. (4) and (12); results are listed in Table 1. It is evident from this table that $\alpha \mapsto F(\alpha)$ is a monotonically decreasing

function of α. Therefore, from Eq. (30), it follows that

$$\omega_{\min} := \frac{0.7071}{(\xi\gamma^*)^{1/2}} = \left(\frac{a_4^2(\infty)}{2a_1(\infty)}\right)^{1/2}\left(\frac{1}{\xi\gamma^*}\right)^{1/2} < \omega_r \leqslant \left(\frac{a_4(0)a_5(0)}{2a_2(0)}\right)^{1/2}\left(\frac{1}{\xi\gamma^*}\right)^{1/2} = \frac{0.8758}{(\xi\gamma^*)^{1/2}} =: \omega_{\max}. \tag{32}$$

From Eq. (12), it is noted that $a_4^2(\alpha)/a_1(\alpha) = 1$ for all $\alpha \geqslant 0$. This fact establishes the greatest lower bound on ω_r in inequality (32). It is concluded from inequality (32) that in the interval $(\omega_{\min}, \omega_{\max}]$, norms $\|g_{\text{tip}}\|_\infty$ corresponding to all beam–mass systems are equal to γ^*. Note that this interval is maximal, is independent of dimensions of the beams and masses of the proof masses, and is inversely proportional to ξ and γ^*.

A major limit of performance of the device in Fig. 6 is apparent from inequality (32). The device does function as a band-pass filter, however, the frequency band $(\omega_{\min}, \omega_{\max}]$, over which the peaks of the Bode magnitude plots of the transfer functions $g_{\text{tip}}(s)$ corresponding to all beam–mass systems remain constant, is limited. This band cannot be widened by changing dimensions of the beams and masses of the proof masses.

Although the device in Fig. 6 as a band-pass filter has limited frequency band, it is necessary to have a systematic procedure to determine dimensions of the beams and masses of the proof masses of such a device. A procedure is given in the following.

Procedure 3.1. Take the following steps to obtain dimensions l, w, and h of the beams and masses of the proof masses M that make the device in Fig. 6 function as a band-pass filter.

Step 1: Choose a $\gamma^* > 0$. Knowing the damping ratio $0 < \xi \ll 1$, obtain the frequency band $(\omega_{\min}, \omega_{\max}]$ from inequality (32).

Step 2: Use the values of α and the corresponding $\lambda(\alpha)$ in Ref. [15, p. 188, Table 6.7(a)] and Eqs. (4) and (12) to compute ω_r from Eq. (30).

Choose a same thickness h for all beams and compute lengths l via Eq. (29), which is written as

$$l = \left(\frac{2a_3(\alpha)}{3a_4(\alpha)[\alpha a_4(\alpha) + a_5(\alpha)]}\right)^{1/4}\left(\frac{E\xi\gamma^*}{\rho}\right)^{1/4} h^{1/2}, \tag{33}$$

for several values of $\alpha \geqslant 0$.

Step 3: Choose a same width w for all beams. Use the chosen w together with h and l from Step 2 to compute masses of the proof masses M from Eq. (28).

A few remarks regarding Procedure 3.1 are in order.

Remarks. (1) By Procedure 3.1, the cantilever beams of the device in Fig. 6 have a same thickness, a same width, but different lengths. It is possible to modify Procedure 3.1 so that the beams would have a same length, a same width, but different thicknesses. Such a procedure results in beams the thicknesses of which differ only slightly from each other. This design is not recommended since beams with slightly different thicknesses are more difficult to fabricate than beams with distinctly different lengths.

(2) Let

$$G(\alpha) := \left(\frac{2a_3(\alpha)}{3a_4(\alpha)[\alpha a_4(\alpha) + a_5(\alpha)]}\right)^{1/4}, \tag{34}$$

for all $\alpha \geqslant 0$. The scalar-valued function $\alpha \mapsto G(\alpha)$ appears on the right-hand side of Eq. (33). This function is evaluated by using the values of α and the corresponding $\lambda(\alpha)$ in Ref. [15, p. 188, Table 6.7(a)] and Eqs. (4) and (12); results are listed in Table 1. It is evident from this table that $\alpha \mapsto G(\alpha)$ is a monotonically decreasing function of α; hence, so is l.

(3) It is possible to compute dimensions of the beams and masses of the proof masses for many values of $\alpha \geqslant 0$ by Procedure 3.1. Such computations, however, are recommended for $\alpha \in [0, 2]$ to avoid proof masses much heavier than the beams. At $\alpha = 2$, it follows from Eq. (30) that $\omega_r = 0.7288/(\xi\gamma^*)^{1/2}$, which is sufficiently close to $\omega_{\min}$.

Next, an example is given to illustrate the application of Procedure 3.1 in designing a mechanical band-pass filter.

Table 2
Dimensions of beams and values of proof masses

Beam	α	Frequency ω_r rad/s (Hz)	l (cm)	w (mm)	h (mm)	M (g)
1	2.00	325.93 (51.87)	3.74	4	0.5	1.5706
2	1.50	328.67 (52.31)	3.97	4	0.5	1.2497
3	1.00	333.56 (53.09)	4.29	4	0.5	0.9005
4	0.75	337.78 (53.76)	4.51	4	0.5	0.7103
5	0.50	344.69 (54.86)	4.80	4	0.5	0.5045
6	0.35	351.41 (55.93)	5.04	4	0.5	0.3706
7	0.25	357.96 (56.97)	5.24	4	0.5	0.2750
8	0.20	362.19 (57.64)	5.35	4	0.5	0.2248
9	0.15	367.32 (58.46)	5.48	4	0.5	0.1728
10	0.10	373.66 (59.47)	5.64	4	0.5	0.1184
11	0.05	381.60 (60.73)	5.82	4	0.5	0.0611
12	0.03	385.30 (61.32)	5.90	4	0.5	0.0372
13	0.00	391.65 (62.33)	6.04	4	0.5	0

Example 3.2. Let the device in Fig. 6 be made out of silver with the properties given in Eqs. (23). In order to determine dimensions of the beams and masses of the proof masses that make this device into a band-pass filter, Procedure 3.1 is used.

Let

$$\gamma^* = 5 \times 10^{-4}\,\mathrm{s}^2. \tag{35}$$

From inequality (32), it follows that

$$(\omega_{\min}, \omega_{\max}] = (316.28, 391.65]\,\mathrm{rad/s} = (50.33, 62.33]\,\mathrm{Hz}. \tag{36}$$

By Step 2 of Procedure 3.1, resonant frequencies ω_r are computed from Eq. (30) for several values of $\alpha \geqslant 0$; they are listed in Table 2. The same thickness $h = 0.0005\,\mathrm{m}$ is chosen for all beams. Then, lengths of the beams are computed via Eq. (33). Results are listed in Table 2 as h and l.

The same width $w = 0.004\,\mathrm{m}$ is chosen for all beams. By Step 3 of Procedure 3.1, masses of the proof masses are computed from Eq. (28); they are tabulated as M in Table 2.

The designed band-pass filter has 13 beam–mass systems. The Bode magnitude plots of the transfer functions $g_{\mathrm{tip}}(s)$ corresponding to these beam–mass systems are shown in Fig. 8. It is evident that all plots have a same peak in the interval $[325.93, 391.65]\,\mathrm{rad/s}$.

4. Conclusions

In this paper, the design of mechanical band-pass filters was studied. Such filters can be used in energy scavengers to convert energy from vibration sources into electricity.

The band-pass filter proposed in this paper is an ensemble of cantilever beams where at the tip of each beam a mass, known as the proof mass, is mounted. A beam with a proof mass at its tip is called the beam–mass system. In order to study the frequency response of such an ensemble, a simple mathematical model was derived to describe the transversal vibration of a beam–mass system. The model is the generalized single-degree-of-freedom (sdof) system corresponding to the beam–mass system. For this model a transfer function was obtained that relates the transversal displacement of the tip of the beam to the acceleration applied by a vibration source. The resonant (fundamental) frequency of this transfer function and its H_∞-norm were obtained in terms of the beam dimensions and the proof mass.

Using the results obtained for one beam–mass system, it was shown that an ensemble of beam–mass systems can be made into a band-pass filter when dimensions of the beams and masses of the proof masses are chosen appropriately. A systematic procedure for designing mechanical band-pass filters was given. Moreover, it was

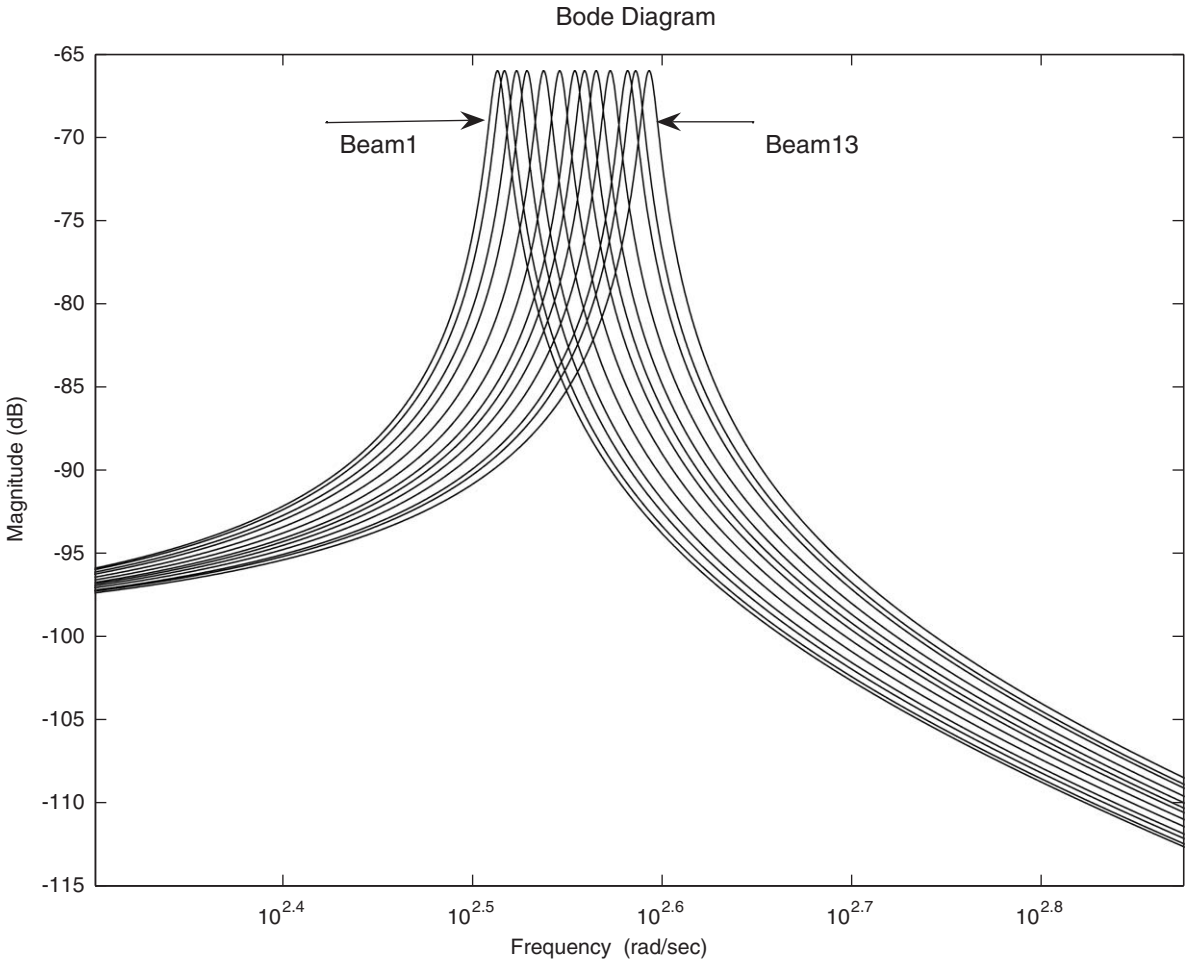

Fig. 8. The Bode magnitude plots of the transfer functions corresponding to the beam–mass systems in Example 3.2. All plots have a same peak in the interval $(\omega_{\min}, \omega_{\max}]$.

shown that the maximal frequency band of the band-pass filter is limited and independent of dimensions of the beams and masses of the proof masses.

Work to design versatile mechanical band-pass filters with reasonable frequency bands over large frequency intervals is in progress. Such filters can be used on a variety of vibration sources with different peak-power frequencies. Results of the ongoing work will be reported in the near future.

References

[1] G. Boyle, B. Everett, J. Ramage (Eds.), *Energy Systems and Sustainability*, Oxford University Press, Oxford, UK, 2003.
[2] W. Shepherd, D.W. Shepherd, *Energy Studies*, second ed., Imperial College Press, London, UK, 2003.
[3] R.M. Dell, D.A.J. Rand, *Clean Energy*, The Royal Society of Chemistry, Cambridge, UK, 2004.
[4] G.M. Masters, *Renewable and Efficient Electric Power Systems*, Wiley, Hoboken, NJ, 2004.
[5] B. Sorensen, *Renewable Energy: Its Physics, Engineering, Use, Environmental Impacts, Economy and Planning Aspects*, third ed., Elsevier Academic Press, Boston, MA, 2004.
[6] C. Shearwood, R.B. Yates, Development of an electromagnetic micro-generator, *Electronics Letters* 33 (22) (1997) 1883–1884.
[7] R. Amirtharajah, A.P. Chandrasakan, Self-powered signal processing using vibration-based power generation, *IEEE Journal of Solid-State Circuits* 33 (5) (1998) 687–695.
[8] S. Meninger, J.O. Mur-Miranda, R. Amirtharajah, A.P. Chandrasakan, J.H. Lang, Vibration-to-electric energy conversion, *IEEE Transactions on Very Large Scale Integration (VLSI) Systems* 9 (1) (2001) 64–76.

[9] N.W. White, P. Glynne-Jones, S.P. Beeby, A novel thick-film piezoelectric micro-generator, *Smart Materials and Structures* 10 (4) (2001) 850–852.
[10] P. Glynne-Jones, S.P. Beeby, N.M. White, Towards a piezoelectric vibration-powered microgenerator, *IEE Proceedings—Science, Measurement and Technology* 148 (2) (2001) 68–72.
[11] P.D. Mitcheson, T.C. Green, E.R. Yeatman, A.S. Holmes, Architectures for vibration-driven micropower generators, *Journal of Microelectromechanical Systems* 13 (3) (2004) 429–440.
[12] Y. Yoshitake, T. Ishibashi, A. Fukushima, Vibration control and electricity generating device using a number of hula-hoops and generators, *Journal of Sound and Vibration* 275 (1–2) (2004) 77–88.
[13] S. Roundy, P.K. Wright, J. Rabaey, *Energy Scavenging for Wireless Sensor Networks: With Special Focus on Vibrations*, Kluwer Academic Publishers, Boston, MA, 2004.
[14] R.W. Clough, J. Penzin, *Dynamics of Structures*, second ed., McGraw-Hill, New York, 1993.
[15] I.A. Karnovsky, O.I. Lebed, *Free Vibration of Beams and Frames*, McGraw-Hill, New York, 2004.
[16] I.S. Gradshteyn, I.M. Ryzhik, *Table of Integrals, Series, and Products*, sixth ed., Academic Press, San Diego, CA, 2000.